Journal of
Nanoscience and Nanotechnology
Vol. 12, 1–5, 2012

Nanoscale Silver-Assisted Wet Etching of Crystalline Silicon for Anti-Reflection Surface Textures

Rui Li[1, 2], Shuling Wang[2], Santhad Chuwongin[2], and Weidong Zhou[2, *]

[1] *Institute of Near-Field Optics and Nano Technology, School of Physics and Optoelectronic Technology, Dalian University of Technology, Dalian 116024, P. R. China*
[2] *Department of Electrical Engineering, University of Texas at Arlington, Arlington, TX 76019, USA*

We report here an electro-less metal-assisted chemical etching (MacEtch) process as light management surface-texturing technique for single crystalline Si photovoltaics. Random Silver nanostructures were formed on top of the Si surface based on the thin film evaporation and annealing process. Significant reflection reduction was obtained from the fabricated Si sample, with ∼2% reflection over a wide spectra range (300 to 1050 nm). The work demonstrates the potential of MacEtch process for anti-reflection surface texture fabrication of large area, high efficiency, and low cost thin film solar cell.

Keywords: Anti-Reflection Coating, Metal-Assisted Chemical Etching, Pyramid, Photovoltaic Cells, Silicon.

RESEARCH ARTICLE

1. INTRODUCTION

Optical design and light trapping are critical in achieving high performance cost effective photovoltaics with for reduced light reflection and improved light absorption.[1–4] Both subtractive etching and additive coating structures have been pursued for anti-reflection (AR) and light trapping.[5–7] However, due to the lack of high index-matched transparent material to Si, the most effective AR structure for high index Si is the surface texturing based on subtractive etching process. The most successful example is the anisotropic etching of single crystal Si (100) surface in a solution containing potassium hydroxide (KOH).[8]

In the past 20 years, porous Si and solar cells studies have become hot topics within science and engineering.[9–12] Porous Si solar cells have some potential benefits on traditional wafer-based or thin-film devices related to optical and electrical effects and cost. We report here an electroless metal-assisted electrochemical etching (MacEtch) process[13–15] as light management surface-texturing technique for single crystalline Si photovoltaics. The MacEtch process is summarized in Figure 1. First, an ultra-thin silver film was deposited on Si surface based on thermal evaporation process. Precise thickness control was achieved by controlling the very low deposition rate (less than 0.1 Å/sec). Silver film coated Si sample was then annealed at 300 °C in a furnace for one hour under nitrogen environment. The silver film was self-assembled to form silver hemi-sphere nano-particles, as shown in Figure 1(b). The increase of the film thickness will increase the radius of particles accordingly. Finally, the Si sample, which was covered with the silver hemi-sphere nano-particles formed by annealing process, was immersed into an aqueous solution containing HF (10%) and H_2O_2 (0.6%) for etching at room temperature. Then the etched samples was quickly rinsed several times in HNO_3 and de-ionized water (1:3 v/v) to remove the silver particles then dipped into de-ionized water, and dried at room temperature. The resultant sample is shown in Figure 1(c).

2. EXPERIMENTAL DETAILS

The Si wafer used in this paper is 300 um thick *p*-type (100) Si (boron doped, 7–13 $\Omega \cdot$cm). Before depositing, the wafer was treated with piranha solution (97% H_2SO_4–30% H_2O_2, 3:1 v/v) for 10 minutes, and in HF (49.9% HF-DI water 4:1 v/v) for 10 minutes.

Different thicknesses silver films on the Si wafer leads to different sizes of silver hemi-sphere nano-particles. Figures 2(a), (c), (e) and (g) show the scanning electron micrographs (SEMs) of the particles obtained with silver film thicknesses of 0.5 nm, 1 nm, 5 nm and 9 nm, respectively. The corresponding nano-structured Si layers, shown in Figures 2(b), (d), (f) and (h), were obtained after etching in HF and H_2O_2 solution for 20 minutes with the silver hemi-sphere nano-particles as the catalyst.

*Author to whom correspondence should be addressed.

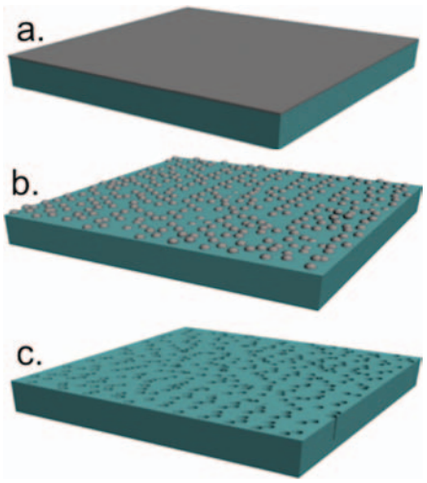

Fig. 1. Schematic illustration of the fabrication process of nano-structured Si: (a) Silver film was deposited on the Si surface; (b) Silver nano-particles were formed after annealing silver film in a furnace; and (c) Si sample after etching in the HF and H_2O_2 solution.

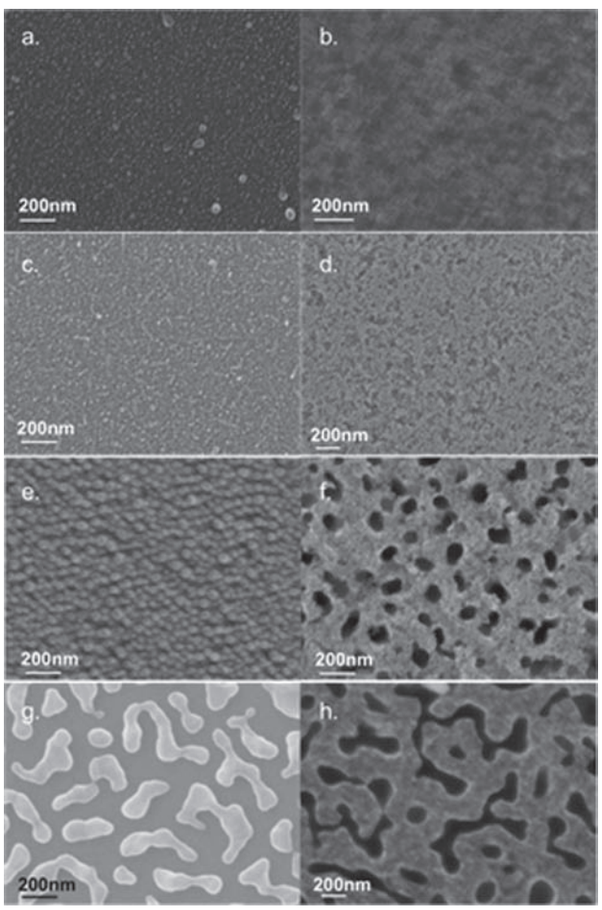

Fig. 2. SEM images (top view) of Si before etching (with silver hemisphere nanoparticles) (left panel) and after etching (right panel). The original silver thin film thicknesses deposited with thermal evaporator are 0.5 nm (a), (b), 1 nm (c), (d), 5 nm (e), (f), and 9 nm (g), (h), respectively.

HF and H_2O_2 can etch the Si surface coated with metal much faster than that without any metal coating.[12] When the Si wafer was dipped into the etchant solution. Si etching rate decreases as the size of the silver nano-hemispheres increases. This is because larger silver nano-hemispheres increase the exchanging path length of HF, H_2O_2, Si and the byproducts. Figure 3 shows the SEM images of the cross-section views of the nano-structure Si with different etching depths under different etching times.

As shown in Figures 2(g), (h) and 3(f), after annealing of thicker silver films, many silver particles connect with each other and form irregular-shaped clusters of different sizes. Thus the etching rate for the silver particles was much different from those hemispherical silver particles. The etching direction was not normal to the surface. With the control of etching time, the etching depth can be

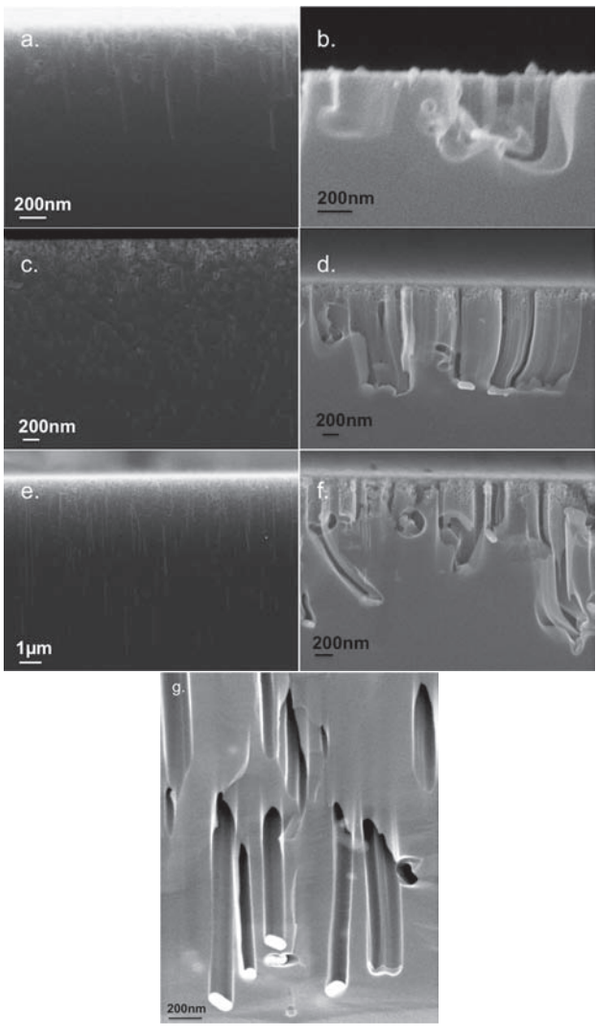

Fig. 3. Cross-sectional SEM images of silver nano-particles with deposited silver film thicknesses of 1 nm (a)–(c), and 9 nm (d)–(f) and different etching times: 2 min (a), (d), 5 min (b), (e), and 20 min (c), (f). A zoom-in SEM image of porous silicon is shown in (g).

RESEARCH ARTICLE

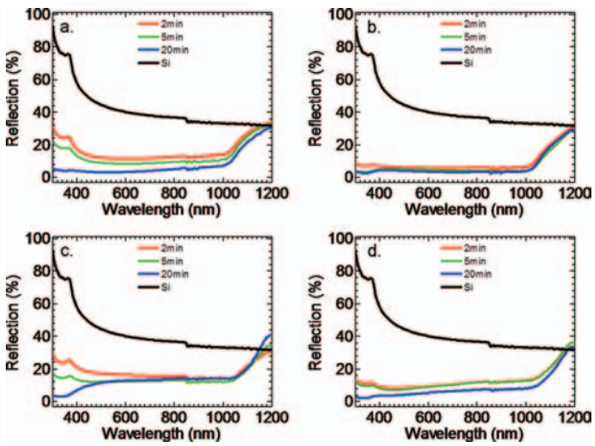

Fig. 4. Measured reflection spectra from nano-structured Si films with different silver film thickness ((a) 0.5 nm, (b) 1 nm, (c) 5 nm, and (d) 9 nm silver film) and different etching times.

controlled from 100 nm to 10 μm. This feature is critical as precise control of etching depth is essential for ultra-thin Si thin films for solar cell applications.

The SEM cross-section view in Figure 3(g) shows well-separated helical cylindrical pores. Silver nano hemi-spheres are found at the bottom of pores, the silver nano hemi-spheres didn't go straightly down to the bottom and they were rotating during etching process, this helical cylindrical structure seems to reduce the reflection of the silicon more effectively than the straight cylindrical etching of the cylindrical pores that were generated by smaller sized sphere metal particles.

Measured reflection spectra are summarized in Figure 4 for nano-structured Si with different silver film thicknesses and different etching times. It is evident that the nano structured Si shows significant reduction in optical reflection than the polished Si over a wide spectral bandwidth of 300–1050 nm, which covers most of the spectrum that is useful for crystalline Si solar cells. The reduction in the reflection is mostly associated with the reduction in the effective index of the nano-structured Si layer, due to the formation of porous Si structure.[16] The weak dependence of the reflection on the nano-structured Si layer thickness (with different etching times) has also been investigated previously,[17] where it was found that for the nano-structured AR structures, the total reflection not only depends on the effective index of the structure, it also depends on the total AR structure thickness and the refractive index change rate (i.e., the index profile). In general, longer etching time leads to lower reflection. The lowest reflection is around 5% and obtained using 0.5 nm silver films and etching for 20 minutes.

In order to get even lower reflection on Si surface, we combine the two different types of etching to form nano-structures (porous Si) on micro-scale surface texturing. Figure 5 shows the fabrication processing flow ((a)–(d)), along with the corresponding SEM images ((e)–(f)). First, the top surface of the bulk Si was randomly etched in 15% KOH solution at 75 °C for 20 min to form pyramid Si, as shown in Figure 5(a) schematically, and in Figure 5(e) with an SEM image. Secondly, 1 nm silver film was deposited on the pyramid by thermal evaporation (Fig. 5(b)), with a deposition rate lower than 0.1 Å/sec. Third, the silver coated pyramid Si sample was then annealed at 300 °C in a furnace for one hour under nitrogen environment.

The nano-scale silver thin film was self-assembly to hemi-spheres nano-particles on the pyramid, as shown in Figures 5(b) and (c). Shown in Figure 5(f) is a SEM image of the silver hemi-sphere nano-particles formed on the top of the pyramid Si. The zoom-in view of silver particles

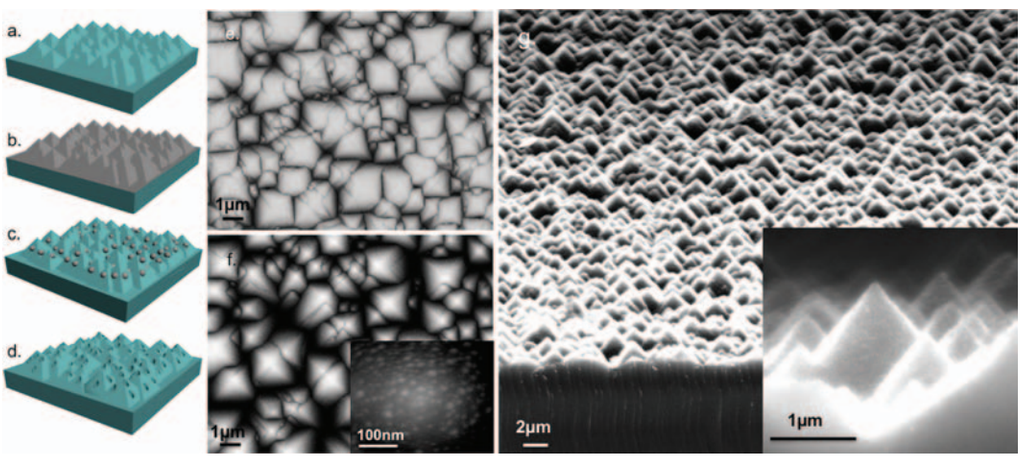

Fig. 5. Schematic illustration of the fabrication process of nano-structured pyramid Si: (a) Random pyramid formatted on the surface of silicon (b) Silver film was deposited on the pyramid Si surface; (c) Silver nano-particles was formed after annealing of silver film in a furnace on the pyramid surface; and (d) Pyramid Si sample after etching in the HF and H_2O_2 solution; and (e) A SEM top view image of the pyramid Si surface; (f) A SEM top view image of the pyramid Si with silver particles, along with a zoom-in SEM image of silver nanoparticles on pyramid Si surface; and (g) A SEM top view image of the porous Si on pyramid Si surface, with inset shown a zoom-in image.

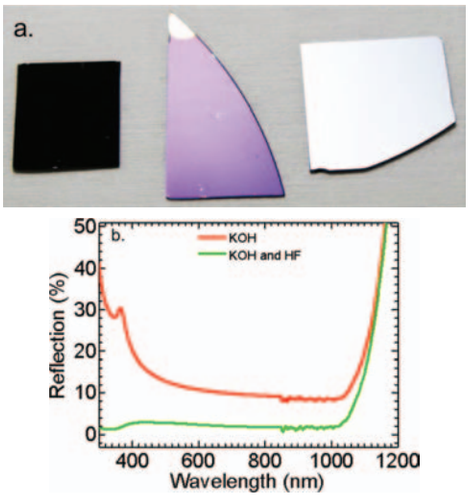

Fig. 6. (a) Photographs of porous pyramid Si (left), SiNx coated Si (middle), and polished crystalline Si (right). (b) Measured reflection spectral results for pyramid Si (with KOH etching only) and for porous pyramid Si (with KOH and HF etching).

formed on the surface of pyramid is shown in the insert of Figure 5(f), indicating the particles were uniform and separate very well for light trapping. Finally, the pyramid wafer covered with the silver hemi-sphere nano-particles was immersed in an aqueous solution containing HF (10%) and H_2O_2 (0.6%) for a 10 min etching at room temperature, as shown schematically in Figure 5(d). Figure 5(g) shows the final structure of the porous pyramid Si.

Figure 6(a) shows photographs of three samples: porous pyramid Si (left), SiNx coated Si (middle), and polished crystalline Si (right). The dark color of the porous pyramid Si indicates very low reflection over the entire visible spectral band. The SiNx coated Si looks purple, indicating low reflection only at certain (narrow) spectral band. The polished Crystalline Si is highly reflective. The reflection measurement result appears over a broad range of wavelengths 300–1200 nm, which covers most of the spectral range that is useful for crystalline Si solar cells. The measured results are shown in Figure 6(b). For the entire spectral band between 300 nm and 1050 nm, the reflection

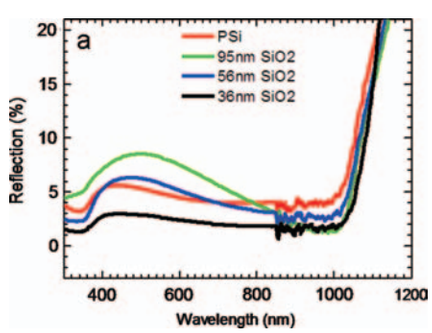

Fig. 7. Measured reflections for nano-structured Si (1 nm silver film thickness, etched for 20 min) coated with different thicknesses of SiO_2.

of the porous pyramid Si was lower than 2%, which is much better than SiNx coated Si. Such low reflection is the results of the follow two effects. First, micro-scale pyramid surface texturing of Si surface can enhance light trapping for increase light path inside Si and reduced reflection over a large spectral range.[18] Secondly, the nano-structured porous Si structure offered graded index configuration for further reduction in reflections.[5] The reflection can be further reduced by depositing a thin layer of SiO_2 on the nano-structured Si, as summarized in Figure 7. Typically, the minimal of the reflection spectral location is determined by the quarter wavelength thickness of the low index (SiO_2) film. The best anti-reflection spectral performance was achieved with an oxide layer thickness of 36 nm.

3. CONCLUSIONS

We report here an electroless metal-assisted electrochemical etching (MacEtch) process as light management surface-texturing technique for single crystalline Si photovoltaics. Random silver nanostructures were formed on the top of the flat Si surface micro- and nano-structured surface texturing of Si were carried out based on MacEtch process. Significant reflection reduction was obtained from the fabricated Si sample, with $\sim 2\%$ reflection over a wide spectra range (300 to 1050 nm). With the control of etching time, etching depth can be controlled from 100 nm to 10 μm. This feature is critical as precise control of etching depth is essential for ultra-thin Si thin films for solar cell applications. The work demonstrates the potential of MacEtch process for the fabrication of large area, high efficiency, and low cost thin film solar cell.

Acknowledgments: Rui Li acknowledges CSC scholarship funding for financial support.

References and Notes

1. M. A. Green, *34th IEEE Photovoltaic Specialists Conference (PVSC) Proceedings* **(2009)**, p 146.
2. K. Catchpole and A. Polman, *Opt. Express* 16, 21793 **(2008)**.
3. M. Agrawal and P. Peumans, *Opt. Express* 16, 5385 **(2008)**.
4. J. L. Cruz-Campa, M. Okandan, P. J. Resnick, P. Clews, T. Pluym, R. K. Grubbs, V. P. Gupta, D. Zubia, and G. N. Nielson, *Sol. Energy Mater. Sol. Cells* 95, 551 **(2011)**.
5. W. Zhou, M. Tao, L. Chen, and H. Yang, *J. Appl. Phys.* 102, 103105 **(2007)**.
6. H. S. Chang and H. C. Jung, *J. Nanosci. Nanotechnol.* 11, 3680 **(2011)**.
7. Y. Wang and W. Zhou, *J. Nanosci. Nanotechnol.* 10, 1563 **(2010)**.
8. D. L. King and M. E. Buck, *22nd IEEE Photovoltaic Specialists Conference Proceedings* **(1991)**, p. 303.
9. T. Tsuboi, T. Sakka, and Y. H. Ogata, *J. Appl. Phys.* 83, 4501 **(1998)**.
10. U. Gruning, V. Lehmann, S. Ottow, and K. Busch, *Appl. Phy. Lett.* 68, 747 **(1996)**.
11. C. Chartier, S. Bastide, and C. Lévy-Clément, *Electrochim. Acta* 53, 5509 **(2008)**.

RESEARCH ARTICLE

12. L. Li, S. Liu, X. Ye, M. Hossu, K. Jiang, W. Chen, and Z. Wang, *J. Nanosci. Nanotechnol.* 12, 3954 **(2012)**.
13. X. Li and P. Bohn, *Appl. Phys. Lett.* 77, 2572 **(2000)**.
14. Z. Huang, N. Geyer, P. Werner, J. De Boor, and U. Gösele, *Adv. Mater.* 23, 285 **(2011)**.
15. X. Li, *Curr. Opin. Solid State Mater. Sci.* 16, 71 **(2012)**.
16. M. Born and E. Wolf, Principles of Optics: Electromagnetic Theory of Propagation, Interference and Diffraction of Light, Cambridge University Press **(1999)**.
17. A. S. Chadha, W. Zhou, and E. D. Cline, *38th IEEE Photovoltaics Specialist Conference Proceedings* **(2012)**, p. 2521.
18. J. Zhao and M. A. Green, *IEEE Trans. Electron Dev.* 38, 1925 **(1991)**.

Received: 30 July 2012. Accepted: 30 October 2012.